



GREEN SYNTHESIS OF SILVER NANOPARTICLES FROM *Cymodocea serrulata* AND ITS ASSESSMENT OF ITS ANTIOXIDANT ACTIVITY

B.N. Poojitha¹, P. Amudha^{1*}, R. Vidya¹, S. Sudhashini¹, V. Rani¹, Taslima Nasreen¹,
M. Jayalakshmi²

¹Department of Biochemistry, Vels Institute of Science, Technology and Advanced Studies,
Pallavaram, Chennai, Tamilnadu-600117.

²Department of Biochemistry, Mahalakshmi Women's College of Arts & Science, Chennai,
Tamilnadu – 600 071

***Corresponding Author**

Dr. P. Amudha

Assistant Professor Department of Biochemistry,
School of Life Sciences, VISTAS, Chennai-600 117.

Email:amudhaa85@gmail.com

Contact No: 7904075676

Orchid ID: <https://orcid.org/0000-0001-6828-9558>

ABSTRACT:

The green synthesis of *Cymodocea serrulata* silver nanoparticles was rendered by using seagrass leaves extract. These extracts acted as a capping and reducing agent in stabilizing the formation of AgNPs. The obtained NPs were characterized by using UV, FTIR, SEM, TEM, EDX and XRD methods. UV–V is spectra of the reaction mixture of silver nitrate solution with extract the peak was observed at 422.30nm indicating the presence of silver nanoparticles. SEM analysis was carried out to understand the topology and the size of the NPs, which showed the synthesis of higher density polydispersed spherical NPs of various sizes that ranged from 22 to 65nm and crystalline nature of the nanoparticles. TEM analysis illustrated the particles are spherical in shape and appear well-dispersed with a size range from 18-65 nm. The EDX elemental analysis of the synthesized silver nanoparticles showed highest proportion by weight of silver (80.22%) followed by Chloride (16.45%) and Oxygen (4.43%). The crystalline nature of AgNPs was further established from X-ray diffraction (XRD) analysis display the XRD pattern of nanoparticles acquired from colloid samples. The antioxidant property of green synthesized AgNPs from *Cymodocea serrulata* extract was determined to be nearest to the IC₅₀ values of standards. This shows the ability of green synthesized AgNPs to scavenge free radicals. The green synthesized AgNPs of *Cymodocea serrulata* can be further exploited as a potential candidate for antioxidant agents.

Keywords: Antioxidant, *Cymodocea serrulata*, Silver Nanoparticle, SEM, TEM, EDX, XRD.

Introduction

The research on marine plants has brought to limelight bioactive natural products produced by them in response to physical, chemical and biological changes in the environment. In folk medicine, seagrass have been used for a variety of remedial purpose, eg: for the treatment of fever and skin disease, muscle pain, wounds and stomach problems, remedy against stings of different kind of rays, tranquilizer for babies and ant cancerous properties (De la Torre-Castro M & Ronnback P, 2004). These bioactive natural products have been proved to have unique pharmacological properties. Hence, the growing interest to find cheap, renewable and abundant sources of antioxidants has fostered research on marine plants. Many of the biological functions of seagrass such as antioxidant property, antiviral, anti-diabetic and Vaso protective; insecticidal and larvicidal activity have been attributed by the higher phenolic content of seagrass tissue. However, research on the antioxidant activity of seagrass has not been much carried out compared to the seaweeds, and initiated only recently [Athiperumalsami T, 2010].

The ongoing nanotechnology revolution afford various applications in the field of medicine, cellular imaging, drug and gene delivery, MRI imaging, cancer cell detection, nano cryosurgery and more importantly cancer therapy (Pandit C, *et al.*, 2022). With these diverse applications of nanoparticle (NP) in medicinal/bio-medical field, one of the areas with special interest is the cellular response of NPs against cancer cells; thereby it can be used for future medicine. Silver NPs (Ag NPs) are well known for its application in medicine as a potential antibacterial agent, inhibition of biofilm, treatment of burns and wounds (Nguyen D.D & Lai, J.-Y, 2022). Use of several plants involved in the green synthesis of many types of nanoparticles (Alhumaydhi F.A, 2022). It is very simple, eco-friendly, non-pollution and less cost techniques. Green synthesized nanoparticles are the most suitable candidates for a several biological and catalytic activity which includes anticancer, antibacterial, antiviral without negative side effects (Arya A. & Chundawat T. S, 2020).

In this study, silver nanoparticles were synthesized from the *Cymodocea serrulata* extract. The seagrass can be found in clear water and in the high intertidal areas. It is a hardy species and it is adaptable to marginal conditions. *Cymodocea serrulata* is widespread in the Indo-Pacific. In the Pacific, it is found from southern Japan to Taiwan to the Philippines, Indonesia, and Malaysia extending throughout the Gulf of Thailand and the coast of Vietnam to Hainan, China. It occurs across insular Southeast Asia to New Caledonia, northern Australia and across Micronesia to the Northern Mariana Islands. This is the first report on the synthesis and characterization of silver nanoparticles from the seagrass *Cymodocea serrulata*, although many eco-friendly production of silver nanoparticles for the drug discovery mechanism has been thoroughly investigated with different plant extracts (Zhang L, 2020). Hence, the following objectives were pursued in this study: (i) green synthesis and characterization of silver nanoparticles from the seagrass *Cymodocea serrulata*; and (ii) evaluation of the antioxidant activities of silver nanoparticles.

MATERIALS AND METHODS

Preparation of extract *Cymodocea serrulata*

Twenty grams of *Cymodocea serrulata* powder sample was mixed into one hundred milliliter of deionized water and the mixture was boiled for 10 min. After cooling the extract was filtered with Whatman No. 1 filter paper. The filtrate was stored at 4°C for further use.

Synthesis of Ag nanoparticles using seagrass extract

Silver nanoparticle synthesized by the method of Arunachalam *et al.*, (2012). In this method, 5 ml of extract was added to 45 ml of 1 mM aqueous AgNO₃ solution in a 250 ml Erlenmeyer flask. The flask was then incubated in the dark at five hours (to minimize the photo activation of silver nitrate), at room temperature. A control setup was also maintained without extract. The AgNPs solution thus attained was purified by repeated centrifugation at 10,000 rpm for 15 min followed by re-dispersion of the pellet in de-ionized water. Then the silver nanoparticles were freeze dried for using characterization analysis.

Characterization of Silver Nanoparticles

UV- Visible Spectroscopy (Arunachalam, *et al.*, 2012)

The silver nanoparticles were examined under UV and visible spectrophotometer analysis. The silver nanoparticles were scanned within the wavelength starting from 200-1000 nm using Perkin Elmer photometer and also the characteristic peaks were identified.

FT-IR Spectroscopic analysis (Arunachalam, *et al.*, 2012)

FTIR analysis was performed using Spectrophotometer system, which was used to detect the characteristic peaks in ranging from 400-4000 cm⁻¹ and their functional groups. The peak values of the UV and FTIR were recorded. Each and every analysis was repeated twice for the spectrum confirmation.

SEM-EDX analysis (P. Magudapathy *et al.*, 2001)

The particle size and morphology of nanoparticles were analysed by ZEEISS-SEM machine. The dried form of silver nanoparticles was sonicated with distilled water, small droplet of silver nanoparticles was placed on glass slide and permitted to dry. The ZEEISS-SEM machine was worked at a vacuum of the order of 10-5 torr. The accelerating voltage is 10 kV. The particle size of nanoparticles can be analyzed by using image magnification software compatible with SEM. Compositional analysis on the sample was carried out by the energy dispersive X-ray spectroscopy (EDS) attached with the SEM. The EDX analysis of Ag sample was done by the SEM machine.

TEM Analysis (Sun Y and Xia Y, 2002)

Transmission electron microscopy (TEM) technique was used to visualize the morphology of the AgNPs. The make of the Transmission electron microscope (TEM; Philips model CM200) technique was to visualize the morphology of nanoparticles. The instrument was operated at an accelerating voltage of 200 kV with ultra-high-resolution of 0.2 nm and magnification of 2,000,000 X. TEM's grid size is 3 mm diameter which was prepared placing 5 µl of the silver nanoparticles solutions on carbon-coated copper grids and drying under mercury lamp and then analyzed.

XRD Analysis (Bykkam *et al.*, 2015)

The X-ray diffraction (XRD) distribution of silver nanoparticles was acquired using an X'Pert Pro X-ray diffractometer that generated Cu K α radiation (with an angular

resolution of 1.5418 angstrom). It is being employed to evaluate the crystalline particle sizes that have been manufactured. At room temperature, X-ray generators were running at a voltage of 40 kV and applying a current of 30 mA to the target. Temperature-dependent strengths were recorded at ambient temperature in steps of 0.05, throughout a range of 25 to 800° C, with the diffractometer attached to a computer for data collection and characterization displays. The scanning of biosynthesized silver nanoparticles exercised in 2θ region and the data is analyzed.

***In vitro* Anti-oxidant Assays:**

DPPH radical-scavenging activity was determined by the method of Shimada, *et al.*, (1992). The superoxide anion radicals scavenging activity was measured by the method of Liu *et al.*, (1997). The scavenging activity for hydroxyl radicals was measured with Fenton reaction by the method of Yu *et al.* (2004). The chelating activity of the *Cymodocea serrulata* extract for ferrous ions Fe²⁺ was measured according to the method of Dinis *et al.*, (1994). Determination of Nitric oxide radical scavenging by Garrat (1964) method.

Statistical Analysis

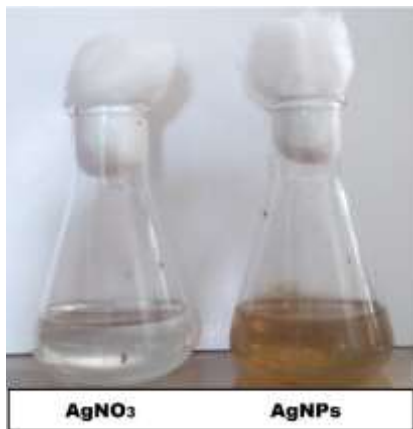
Tests were carried out in triplicate for 3 separate experiments. The amount of extract needed to inhibit free radicals' concentration by 50% (IC₅₀), was graphically determined by a linear regression method using Ms- Windows based graphpad Instat (version 3) software. Results were expressed as graphically/mean ± standard deviation.

RESULTS & DISCUSSION:

The present study deals with the green synthesis of silver nanoparticles, characterization and assessment of antioxidant activity. The AgNPs were synthesized using the extract of seagrass *cymodocea serrulata*. Seagrass is an excellent source of secondary metabolites of pharmacologically important when compared to microorganisms, henceforth it provides the greater scope for the production of biocompatible nanoscale particles. Further, it reveals the biological reduction of silver salt and the formation of silver nanoparticles with surface capping of seagrass metabolite constituents (Fig. 1). The findings are discussed below.

Synthesis of silver nanoparticles from the seagrass *Cymodocea serrulata*:

Phytosynthesis of Ag nanoparticles by the aqueous extract was carried out in this work. During the visual observation, silver nitrate incubated with extract showed a colour change from light yellow to brown after 5 hrs whereas no colour change could be observed in silver nitrate without extract. The appearance of brown colour in extract treated flask is clear indication for the formation of Ag nanoparticles.



AgNO₃

: 1 mM AgNO₃ (White colour)

AgNPs

: 1 mM AgNO₃ in the presence of extract after 5 hours of incubation (Brown colour)

Figure 1: Colour changes before (seagrass extract) and after (AgNPs) the process of reduction of Ag⁺ to Ag nanoparticles and control (AgNO₃)

UV-Visible Spectroscopic analysis of *Cymodocea serrulata*

In the UV-V is spectra of the reaction mixture of silver nitrate solution with extract the peak was observed at 422.30nm indicating the presence of silver nanoparticles which is synthesized by the extract. The particle size and shape depend on the position of the absorption peak (S. Kandakumar, *et al.*, 2014). The time dependent shift in the peak of absorbance indicated the initiation of reaction and synthesis of silver nanoparticles in large quantity.

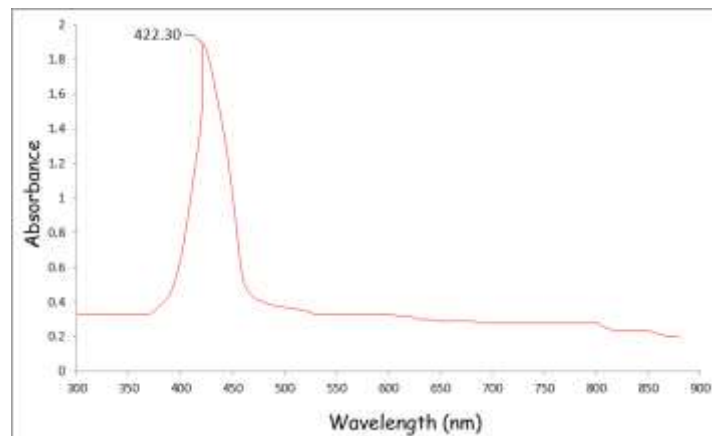


Figure 2: UV-Visible Spectroscopic analysis of AgNPs

FT-IR Spectroscopic Analysis

FTIR spectra were obtained to identify the possible biomolecules in the extract responsible for predicting their role in nanoparticle synthesis and the reduction of silver ions as well as the capping agents responsible for the stability of biogenic nanoparticle solution. The FTIR spectra indicated the existence of various functional groups at different positions (Figure 1 and table 1). The peaks in the region 3449.29cm⁻¹ were assigned to O-H stretching vibration, indicating the presence of hydroxyl groups such as alcohol and phenol compounds while the peaks around 1638, 1400, 1108 and 664 cm⁻¹ corresponds to amines, aromatic (2,

24) and alkenes. The appearance of biomolecules in the extract confirmed their responsibility for the reduction, capping and stabilization of the newly formed nanoparticles

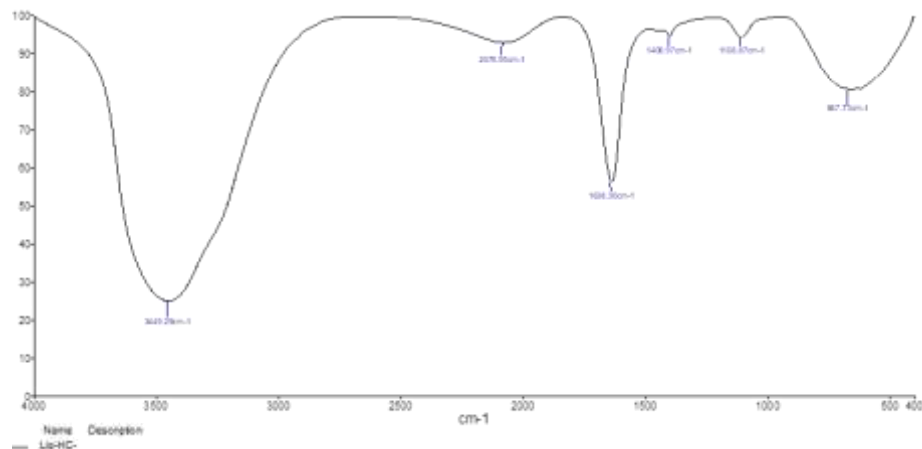


Figure 3: FTIR Spectroscopic analysis of AgNPs

Table 1: Functional group analysis of AgNPs Using FTIR data

Frequency (cm ⁻¹)	Bond	Functional group
3449.29	O-H stretch, H-bonded	Alcohols, Phenols
1638.30	N-H bend	1° amines
1400.97	C-C stretch (in-ring)	Aromatics
1108.87	C-N stretch	Aliphatic amines
667.73	=C-H bend	Alkenes

Scanning Electron Microscopical (SEM) and Particle size analysis

SEM analysis was carried out to understand the topology and the size of the NPs, which showed the synthesis of higher density polydispersed spherical NPs of various sizes that ranged from 22 to 65nm and crystalline nature of the nanoparticles. Most of the nanoparticles gathered and only a little of them were dispersed, when observed under SEM.

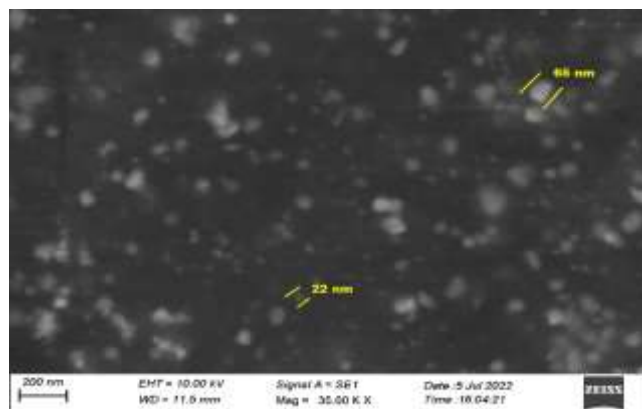


Figure 3: Scanning Electron Microscopical (SEM) analysis of NPs

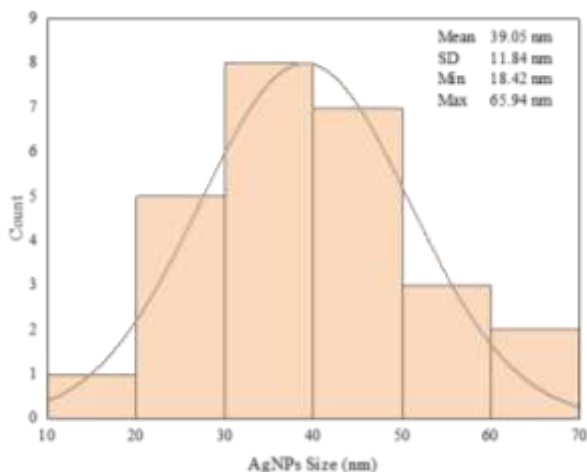


Figure 4: Histogram showing particle size distribution of NPs

To find out the particle size of the nanoparticles using histograms plotted on the obtained data to study the particle size distribution using ImageJ software and the size of the nanoparticles ranged from 18.42 to 65.94 nm and the average particle size was found to be 39.05 ± 11.84 nm. Overall Particle size of NPs were highly distributed between 30nm to 40nm range which is the evidence that the NPs synthesized less than 100nm (NPs < 100nm).

TEM Analysis

TEM provides improved spatial resolution compared with SEM and enables a more in-depth analysis of nanoparticles. The TEM images of colloid nanoparticles are shown in Figure 5. It is observed that the morphology of nanoparticles is often polydispersed and spherical in shape. The synthesized AgNPs were in the range of 18-65 nm. Many researchers have reported that the particle size is controlled by the plant extract. The descriptive images of the AgNPs with their size and structural details are illustrated by the researchers (B. Ajitha, *et al.*, 2015 & Y. Rout, *et al.*, 2012) using TEM analysis.

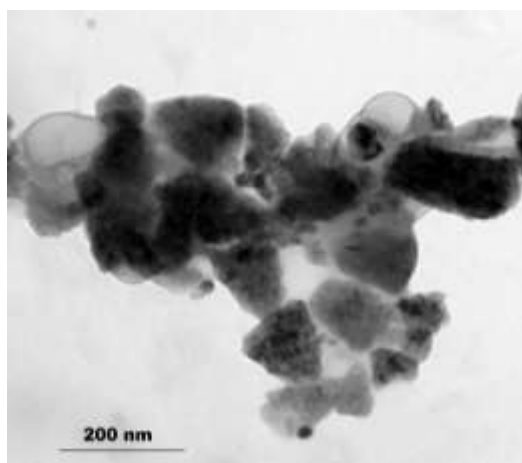


Figure 5: Transmission Electron Microscopical (SEM) analysis of AgNPs

XRD pattern of Ag NPs

XRD is generally used for determining the chemical constituents and crystal structure of a material. The identifying the presence of AgNPs in the sample can be achieved by using XRD to study the diffraction peaks of the AgNPs. X-ray diffraction pattern of AgNPs from the sample extract is shown in Fig. 6. The crystalline nature of AgNPs was further established from X-ray diffraction (XRD) analysis display the XRD pattern of nanoparticles acquired from colloid samples. A number of Bragg reflections with 2ϕ values of 32.15, 38.02, 44.68, 64.76 and 77.11° indicate the (111), (200), (210), (310) and (320) reflections of metallic silver visibly representing the crystalline spherical structure of silver which was associated with the standard powder diffraction card of JCPDS, silver file No. 04-0783. Here, the constant is 29.43 ($106.10 - 76.67 = 29.43$). The unassigned peaks could be due to the crystallization of bioorganic phase that occurs on the surface of the nanoparticle. The reduction of silver ions due to phytochemicals present in the seagarss extract. The findings of obtaining Braggs reflection planes at resulted diffraction peaks for silver nanoparticles are studied (B. Ajitha, *et al.*, 2015 & J.H. Qingbiao, *et al.*, 2007). Hence XRD pattern in the present study showed the crystalline nature of silver nanoparticles. The line broadening of peaks is mainly due to small particle size. Indexing has been done and data are in table 2.

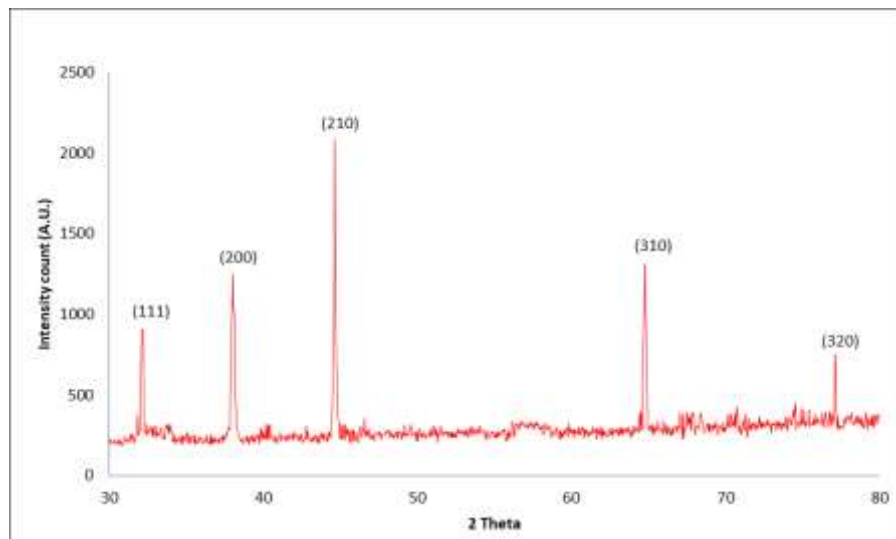


Fig. 6: XRD pattern of silver nanoparticles

Table. 2: Simple peak indexing

Peak position 2θ	$1000 \times$ Sin 2θ	$1000 \times$ Sin $2\theta / 29.43$	Reflection	Remarks
32.15	76.67	3	111	$1^2 + 1^2 + 1^2 = 3$
38.02	106.10	4	200	$2^2 + 0^2 + 0^2 = 4$
44.68	144.47	5	210	$2^2 + 1^2 + 0^2 = 5$
64.76	286.79	10	310	$3^2 + 1^2 + 0^2 = 10$
77.11	388.46	13	320	$3^2 + 2^2 + 0^2 = 13$

Particle Size Calculation

From this study, the peak at degrees and average particle size has been assessed by Debye-Scherrer formula (Bykkam *et al.*, 2015, Nath *et al.*, 2007, Sun *et al.*, 2002).

$$D = 0.9 \lambda / \beta \cos \theta$$

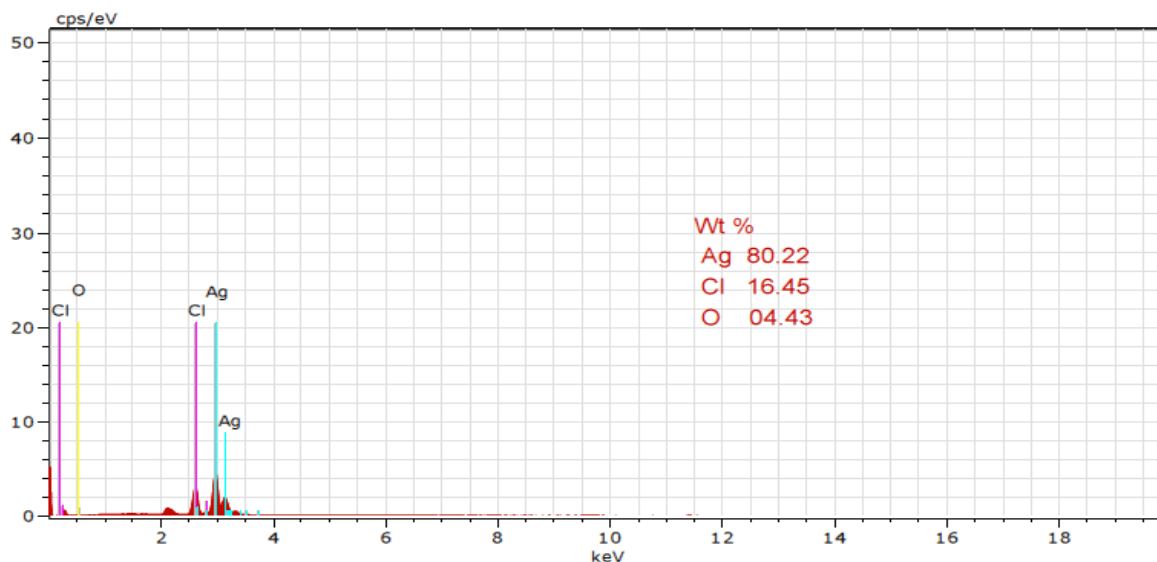
Where ‘λ’ is wave length of X-Ray (0.1541 nm), ‘β’ is FWHM (Full Width at Half Maximum), ‘θ’ is the diffraction angle and ‘D’ is particle diameter size. The average crystalline size according to Debye–Scherrer equation calculated is found to be 24.04nm and represent in table 3.

Table. 3: The grain size of silver Nanoparticles

2θ of the intense peak (deg)	Miller indices (hkl)	θ of the intense peak (deg)	FWHM of intense peak (β) radians	Size of the particle (D) nm
32.15	111	16.075	0.2805	30.96
38.02	200	19.01	0.3317	24.65
44.68	210	22.34	0.3899	21.72
64.76	310	32.38	0.5651	24.78
77.11	320	38.555	0.6729	18.09
Average nanoparticle size				24.04

Energy Dispersive X-Ray Analysis (EDX) analysis

The assessment of the elemental composition on the surface of the biosynthesized nanomaterials was done using EDX spectroscopy. EDX peaks corresponding to element silver show the presence of silver as the ingredient element and the formation and purity of silver nanoparticles synthesized from extract. The EDX elemental analysis of the synthesized silver nanoparticles showed highest proportion by weight of silver (80.22%) followed by



Chloride (16.45%) and Oxygen (4.43%) (Figure 7).

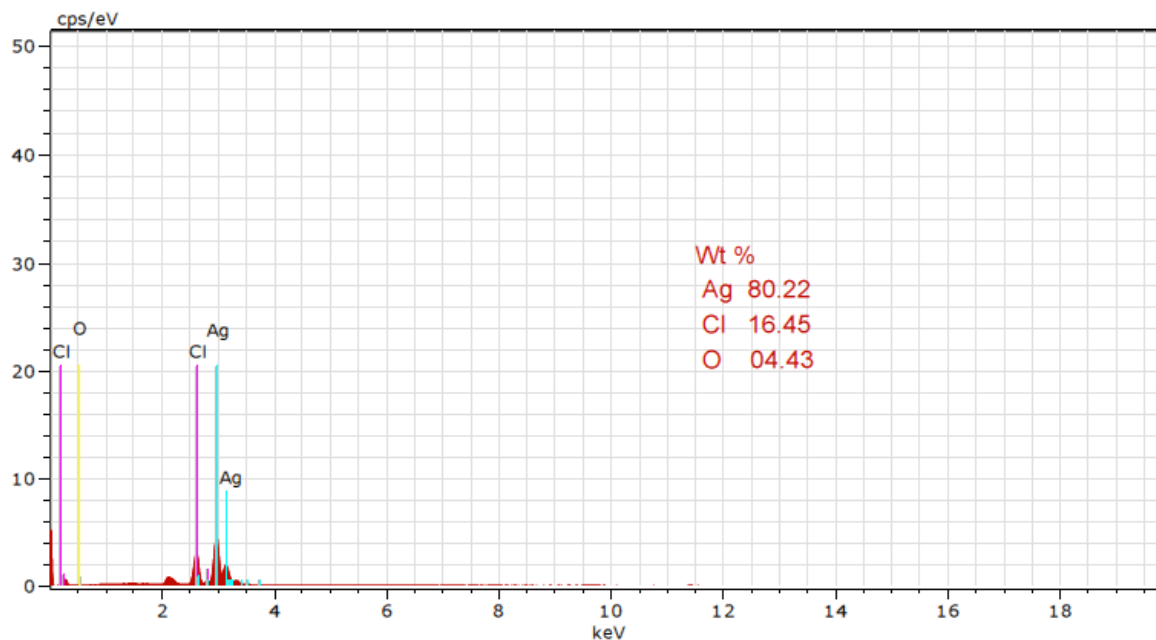


Figure 7 EDX spectrum of AgNPs

IN VITRO ANTIOXIDANT ACTIVITY

DPPH radical scavenging activity

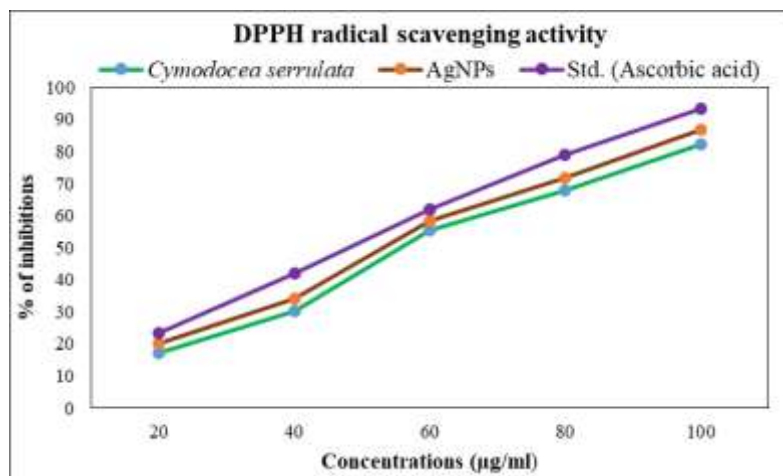
DPPH radical scavenging activity of *Cymodocea serrulata*, AgNPs and compared with ascorbic acid. The *Cymodocea serrulata*, AgNPs and ascorbic acid showed the minimum DPPH inhibitory activity in 20 μ g/ml concentration range (17.13%, 20.27% and 23.42% were *Cymodocea serrulata*, AgNPs and ascorbic acid respectively) while maximum inhibitory activity in 100 μ g/ml concentration range (82.16%, 86.71 and 93.35% were *Cymodocea serrulata*, AgNPs and ascorbic acid respectively) were observed. The half inhibition concentration (IC_{50}) of *Cymodocea serrulata*, AgNPs and ascorbic acid were 59.25 μ g/ml, 54.99 μ g/ml and 48.77 μ g/ml respectively (table 4 & Graph 1). Our study reveals that the synthesized AgNP's particles possessed free radical scavenging activity (C. Dipankar and S. Murugan, 2012). There are number of studies carried by researchers in nanotechnology field on several medicinal plants, but no study is available on synthesis of nanoparticle in *Cymodocea serrulata*. Hence, the attempt was aimed to study the potentiality of *Cymodocea serrulata* mediated nanoparticles for its antioxidant activity. AgNPs has potential DPPH activity than *Cymodocea serrulata* and near to standard. We reported earlier (N.Pushpabharathi, et al., 2019) that the plant *Cymodocea serrulata* is a good source of phenolic compounds and flavonoids.

Table 4: DPPH radical scavenging activity of *Cymodocea serrulata*, AgNPs and compared with standard Ascorbic acid

Concentrations ($\mu\text{g/ml}$)	<i>Cymodocea serrulata</i>		AgNPs		Std. (Ascorbic acid)	
	Absorbance	% of inhibitions	Absorbance	% of inhibitions	Absorbance	% of inhibitions
20	0.237	17.13 \pm 0.06	0.228	20.27 \pm 0.09	0.219	23.42 \pm 0.14
40	0.199	30.41 \pm 0.11	0.188	34.26 \pm 0.18	0.166	41.95 \pm 0.37
60	0.127	55.59 \pm 0.27	0.119	58.39 \pm 0.34	0.109	61.88 \pm 0.46
80	0.092	67.83 \pm 0.49	0.081	71.67 \pm 0.51	0.060	79.02 \pm 0.78
100	0.051	82.16 \pm 0.62	0.038	86.71 \pm 0.79	0.019	93.35 \pm 0.91
IC_{50} ($\mu\text{g/ml}$)	59.25		54.99		48.77	

Values were expressed as mean \pm Standard deviation for triplicates;

IC: Inhibitions concentration; Control absorbance: 0.286

**Graph 1: DPPH radical scavenging activity of *Cymodocea serrulata*, AgNPs and compared with standard ascorbic acid**

Superoxide anion scavenging activity

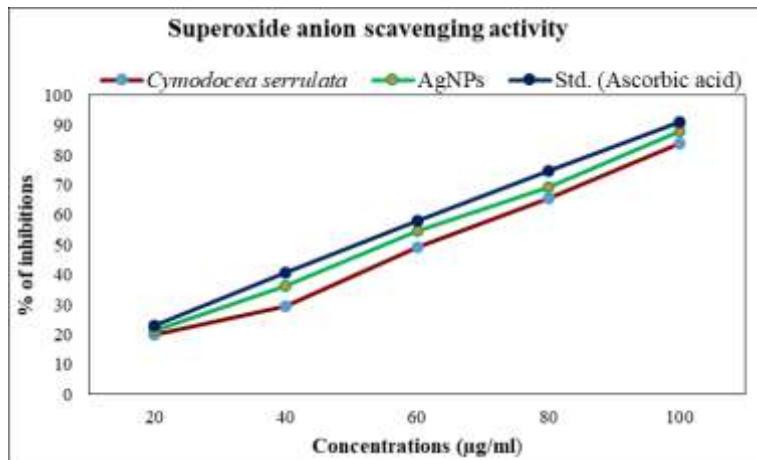
Superoxide anion radical scavenging activity of *Cymodocea serrulata*, AgNPs and compared with ascorbic acid. The *Cymodocea serrulata*, AgNPs and ascorbic acid showed the minimum superoxide anion scavenging inhibitory activity in 20 $\mu\text{g/ml}$ concentration range (19.90%, 21.39% and 22.88% were *Cymodocea serrulata*, AgNPs and ascorbic acid respectively) while maximum inhibitory activity in 100 $\mu\text{g/ml}$ concentration range (84.07%, 88.05 and 91.04% were *Cymodocea serrulata*, AgNPs and ascorbic acid respectively) were observed. The half inhibition concentration (IC_{50}) of *Cymodocea serrulata*, AgNPs and ascorbic acid were 60.42 $\mu\text{g/ml}$, 55.27 $\mu\text{g/ml}$ and 51.18 $\mu\text{g/ml}$ respectively (table 5 & Graph 2). AgNPs has potential superoxide anion scavenging activity than *Cymodocea serrulata* and near to standard.

Table 5: Superoxide anion scavenging activity of *Cymodocea serrulata*, AgNPs and compared with standard ascorbic acid

Concentrations ($\mu\text{g/ml}$)	<i>Cymodocea serrulata</i>		AgNPs		Std. (Ascorbic acid)	
	Absorbance	% of inhibitions	Absorbance	% of inhibitions	Absorbance	% of inhibitions
20	0.161	19.90 \pm 0.15	0.158	21.39 \pm 0.19	0.155	22.88 \pm 0.21
40	0.142	29.35 \pm 0.28	0.128	36.31 \pm 0.33	0.119	40.79 \pm 0.42
60	0.102	49.25 \pm 0.43	0.091	54.72 \pm 0.57	0.084	58.20 \pm 0.61
80	0.069	65.67 \pm 0.59	0.062	69.15 \pm 0.62	0.051	74.62 \pm 0.88
100	0.032	84.07 \pm 0.72	0.024	88.05 \pm 0.91	0.018	91.04 \pm 1.02
IC_{50} ($\mu\text{g/ml}$)	60.42		55.27		51.18	

Values were expressed as mean \pm Standard deviation for triplicates;

IC: Inhibitions concentration; Control absorbance: 0.201

**Graph 2: Superoxide anion scavenging activity of *Cymodocea serrulata*, AgNPs and compared with standard ascorbic acid**

Hydroxyl radical scavenging activity

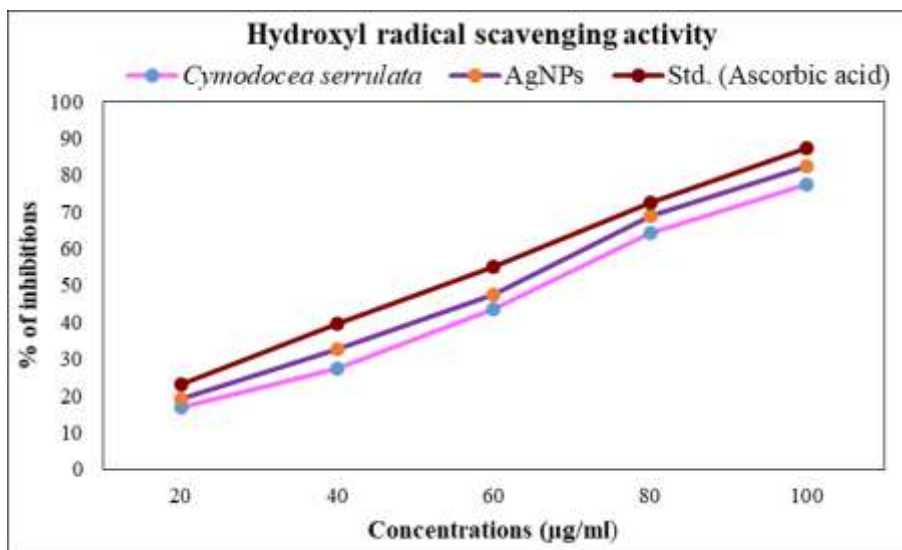
Hydroxyl radical scavenging activity of *Cymodocea serrulata*, AgNPs and compared with ascorbic acid. The *Cymodocea serrulata*, AgNPs and ascorbic acid showed the minimum hydroxyl radical scavenging inhibitory activity in 20 $\mu\text{g/ml}$ concentration range (16.84%, 19.04% and 23.07% were *Cymodocea serrulata*, AgNPs and ascorbic acid respectively) while maximum inhibitory activity in 100 $\mu\text{g/ml}$ concentration range (77.28%, 82.41 and 87.17% were *Cymodocea serrulata*, AgNPs and ascorbic acid respectively) were observed. The half inhibition concentration (IC_{50}) of *Cymodocea serrulata*, AgNPs and ascorbic acid were 65.26 $\mu\text{g/ml}$, 59.87 $\mu\text{g/ml}$ and 53.23 $\mu\text{g/ml}$ respectively (table 6 & Graph 3). AgNPs has potential hydroxyl radical scavenging activity than *Cymodocea serrulata* and near to standard.

Table 6: Hydroxyl radical scavenging activity of *Cymodocea serrulata*, AgNPs and compared with standard ascorbic acid

Concentrations ($\mu\text{g/ml}$)	<i>Cymodocea serrulata</i>		AgNPs		Std. (Ascorbic acid)	
	Absorbance	% of inhibitions	Absorbance	% of inhibitions	Absorbance	% of inhibitions
20	0.227	16.84 \pm 0.07	0.221	19.04 \pm 0.13	0.21	23.07 \pm 0.20
40	0.198	27.47 \pm 0.19	0.184	32.60 \pm 0.26	0.165	39.56 \pm 0.31
60	0.154	43.58 \pm 0.32	0.143	47.61 \pm 0.49	0.123	54.94 \pm 0.50
80	0.098	64.10 \pm 0.67	0.085	68.86 \pm 0.70	0.075	72.52 \pm 0.78
100	0.062	77.28 \pm 0.71	0.048	82.41 \pm 0.87	0.035	87.17 \pm 0.95
IC_{50} ($\mu\text{g/ml}$)	65.26		59.87		53.23	

Values were expressed as mean \pm Standard deviation for triplicates;

IC: Inhibitions concentration; Control: 0.273

**Graph 3: Hydroxyl radical scavenging activity of *Cymodocea serrulata*, AgNPs and compared with standard ascorbic acid****Iron (Fe^{2+}) chelating activity**

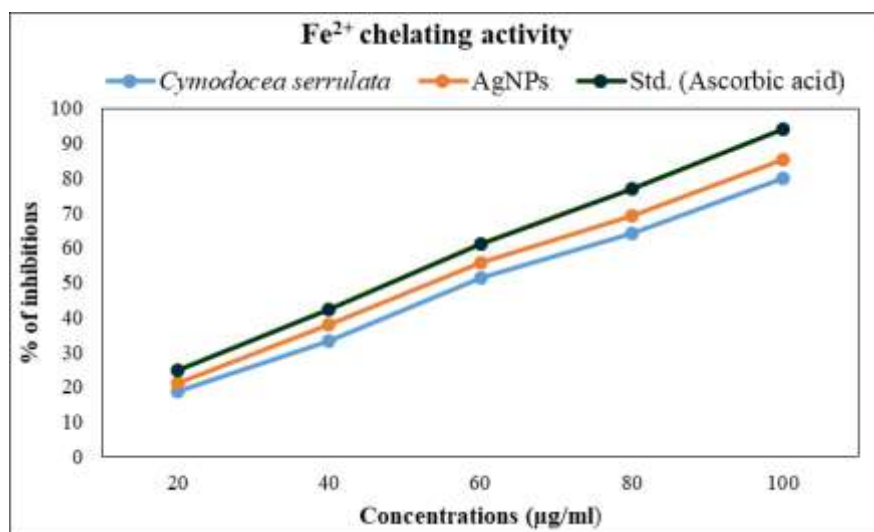
Fe^{2+} chelating activity of *Cymodocea serrulata*, AgNPs and compared with ascorbic acid. The *Cymodocea serrulata*, AgNPs and ascorbic acid showed the minimum Fe^{2+} chelating inhibitory activity in 20 $\mu\text{g/ml}$ concentration range (18.58%, 20.94% and 24.66% were *Cymodocea serrulata*, AgNPs and ascorbic acid respectively) while maximum inhibitory activity in 100 $\mu\text{g/ml}$ concentration range (80.06%, 85.47 and 93.91% were *Cymodocea serrulata*, AgNPs and ascorbic acid respectively) were observed. The half inhibition concentration (IC_{50}) of *Cymodocea serrulata*, AgNPs and ascorbic acid were 60.70 $\mu\text{g/ml}$, 55.20 $\mu\text{g/ml}$ and 48.70 $\mu\text{g/ml}$ respectively (table 7 & graph 4). AgNPs has potential Fe^{2+} chelating activity than *Cymodocea serrulata* and near to standard.

Table 7: Fe²⁺ chelating activity of *Cymodocea serrulata*, AgNPs and compared with standard ascorbic acid

Concentrations ($\mu\text{g/ml}$)	<i>Cymodocea serrulata</i>		AgNPs		Std. (Ascorbic acid)	
	Absorbance	% of inhibitions	Absorbance	% of inhibitions	Absorbance	% of inhibitions
20	0.241	18.58 \pm 0.06	0.234	20.94 \pm 0.12	0.223	24.66 \pm 0.19
40	0.198	33.10 \pm 0.18	0.184	37.83 \pm 0.34	0.171	42.22 \pm 0.36
60	0.144	51.35 \pm 0.38	0.131	55.74 \pm 0.55	0.115	61.14 \pm 0.61
80	0.106	64.18 \pm 0.64	0.091	69.25 \pm 0.71	0.068	77.02 \pm 0.77
100	0.059	80.06 \pm 0.79	0.043	85.47 \pm 0.90	0.018	93.91 \pm 1.04
IC ₅₀ ($\mu\text{g/ml}$)	60.70		55.20		48.70	

Values were expressed as mean \pm Standard deviation for triplicates;

IC: Inhibitions concentration; Control absorbance: 0.296

**Graph 4: Fe²⁺ chelating activity of *Cymodocea serrulata*, AgNPs and compared with standard Ascorbic acid**

Nitric oxide scavenging activity

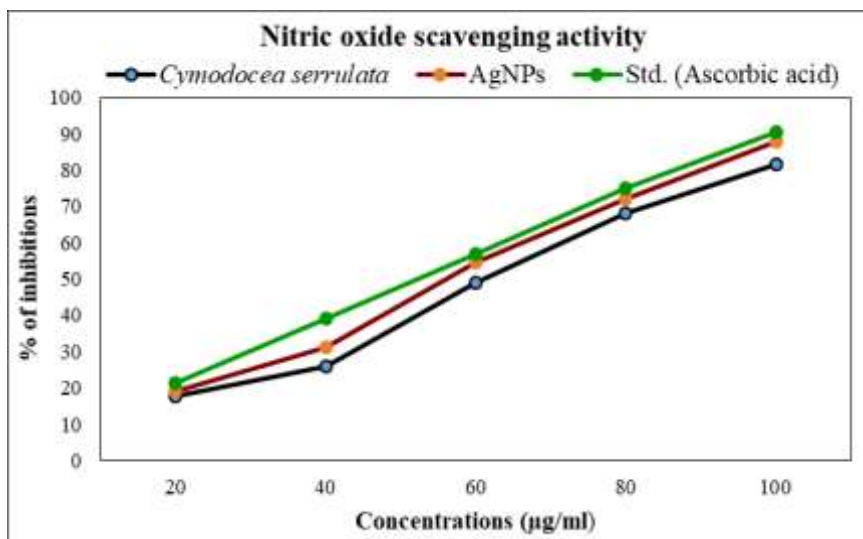
Nitric oxide scavenging activity of *Cymodocea serrulata*, AgNPs and compared with ascorbic acid. The *Cymodocea serrulata*, AgNPs and ascorbic acid showed the minimum nitric oxide scavenging inhibitory activity in 20 $\mu\text{g/ml}$ concentration range (17.58%, 19.13% and 21.29% were *Cymodocea serrulata*, AgNPs and ascorbic acid respectively) while maximum inhibitory activity in 100 $\mu\text{g/ml}$ concentration range (81.58%, 87.72 and 90.61% were *Cymodocea serrulata*, AgNPs and ascorbic acid respectively) were observed. The half inhibition concentration (IC₅₀) of *Cymodocea serrulata*, AgNPs and ascorbic acid were 61.74 $\mu\text{g/ml}$, 56.72 $\mu\text{g/ml}$ and 52.44 $\mu\text{g/ml}$ respectively (table 8 & graph 5). AgNPs has potential nitric oxide scavenging activity than *Cymodocea serrulata* and near to standard.

Table 8: Nitric oxide scavenging activity of *Cymodocea serrulata*, AgNPs and compared with standard ascorbic acid

Concentrations ($\mu\text{g/ml}$)	<i>Cymodocea serrulata</i>		AgNPs		Std. (Ascorbic acid)	
	Absorbance	% of inhibitions	Absorbance	% of inhibitions	Absorbance	% of inhibitions
20	0.228	17.68 \pm 0.08	0.224	19.13 \pm 0.20	0.218	21.29 \pm 0.23
40	0.205	25.99 \pm 0.22	0.191	31.04 \pm 0.34	0.169	38.98 \pm 0.37
60	0.141	49.09 \pm 0.48	0.126	54.51 \pm 0.59	0.119	57.03 \pm 0.67
80	0.088	68.23 \pm 0.59	0.077	72.20 \pm 0.66	0.069	75.09 \pm 0.81
100	0.051	81.58 \pm 0.73	0.034	87.72 \pm 0.85	0.026	90.61 \pm 1.01
IC_{50} ($\mu\text{g/ml}$)	61.74		56.72		52.44	

Values were expressed as mean \pm Standard deviation for triplicates;

IC: Inhibitions concentration; Control absorbance: 0.277

**Graph 5:** Nitric oxide scavenging activity of *Cymodocea serrulata*, AgNPs and compared with standard ascorbic acid

Conclusion:

Herein, we demonstrated that the extract of the *Cymodocea serrulata* is capable of production, AgNPs extracellularly by rapid reduction of silver ions. On the basis of the study results obtained it can be found that the approach to phytosynthesis of AgNP's from seagrass extract of *Cymodocea serrulata* is simple, less cost, precise and environmentally friendly approach. It is fast and convenient method. As *Cymodocea serrulata* seagrass extract has great medicinal importance and on other hand, AgNP's are potentially biocompatible, the results depicted here will be useful in pharmacological applications and further research in the field of nanobiotechnology. A color changes from light to yellowish to reddish to colloidal during the formation of silver nanoparticles is confirmed by UV–Vis spectroscopy and characterization was done using, SEM, XRD, FTIR and TEM analysis. The antioxidant activity of biologically synthesized AgNPs and seagrass extract was evaluated by antioxidant assay revealed the scavenging ability for free radicals. Therefore, green synthesis is more

economic and advantage to produce promising and compatible metal nanoparticles using biological method at commercial level and to explore their potentials in drug delivery system using surface capping activities of medicinally useful herbal metabolites.

REFERENCES:

1. Alhumaydhi, F.A. (2022). Green Synthesis of Gold Nanoparticles Using Extract of *Pistacia chinensis* and Their In Vitro and In Vivo Biological Activities. *J. Nanomater*, 5544475.
2. Arunachalam, R., Dhanasingh, S., Kalimuthu, B., Uthirappan, M., Rose, C., and Asit Baran, M. (2012). Phytosynthesis of silver nanoparticles using *Coccinia grandis* leaf extract and its application in the photocatalytic degradation. *Colloids and Surfaces B, Biointerfaces*, 94, 226– 230.
3. Athiperumalsami, T., Devi Rajeswari, V., Hastha Poorna, S., Kumar, V. and Louis Jesudass V. (2010). Antioxidant activity of seagrasses and seaweeds. *Bot Mar*, 53(3), 251-7.
4. B. Ajitha, Y. AK. Reddy and P.S. Reddy. (2015). Green synthesis and characterization of silver nanoparticles using *Lantana camara* leaf extract. *Materials Science and Engineering C*, 49, 373–381.
5. Bykkam, S., Mohsen Ahmadipour., Sowmya Narisngam., Venkateswara Rao Kalagadda., & Shilpa Chakra Chidurala. (2015). Extensive Studies on X-Ray Diffraction of Green Synthesized Silver Nanoparticles. *Advances in Nanoparticles*, 4, 1-10.
6. Dipankar, C. and Murugan. S. (2012). The green synthesis, characterization and evaluation of the biological activities of silver nanoparticles synthesized from *Iresine herbstii* leaf aqueous extracts. *Colloids and Surfaces B: Biointerfaces*, 98, 112–119.
7. De la Torre-Castro, M., Ronnback, P. (2004). Links between humans and seagrasses - An example from tropical East Africa. *Ocean and Coas Manag*, 47(7), 361-87.
8. Dinis, T. C. P., Madeira, V. M. C., Almeidam, L. M. (1994). Action of phenolic derivates (acetoaminophen, salicylate, and 5-aminosalicylate) as inhibitors of membrane lipid peroxidation and peroxy radical scavengers. *Achieves of Biochemistry and Biophysics*, 315, 161-169.
9. Garrat, D.C. (1964). The quantitative analysis of drugs, Japan: Chapman and Hall. Vol. 3: pp. 456-458.
10. Qingbiao, J.H., Yinghua, L.D., Yuanbo, S. L., Yan, S.X., Yuanpeng, H.W., Wenyao, W.S.N. He, Hong, J. and Chen, C. (2007). Biosynthesis of silver and gold nanoparticles by novel sundried *Cinnamomum camphora* leaf. *Nanotechnology*, 18, 1 -11.
11. Liu, F., Ooi, C.V.E. and Chang, S.T. (1997). Free radical scavenging activity of mushroom polysaccharide extracts. *Life Sci*, 60, 763-771.

12. Pushpa Bharathi, N., Jayalakshmi, M., Amudha, P. and Vanitha, V. (2019). Phytochemical screening and *invitro* antioxidant activity of the seagrass *Cymodocea serrulata*. Indian Journal of Geo Marine Sciences, 48(08), 1216-1221.
13. Nath, S. S., Chakdar, D., & Gope, G. (2007). Synthesis of CdS and ZnS Quantum Dots and Their Applications in Electronics. Nanotrends A Journal of Nanotechnology and Its Application, 2, 3.
14. Nguyen, D.D. and Lai, J.Y. (2022). Synthesis, bioactive properties, and biomedical applications of intrinsically therapeutic nanoparticles for disease treatment. Chem. Eng. J., 435, 134970.
15. Magudapathy, P., Gangopadhyay, P., Panigrahi, B.K., Nair, K.G.M. and Dhara, S. Physica B, (2001). 299, 142.
16. Pandit, C., Roy, A., Ghotekar, S., Khusro, A., Islam, M.N., Emran, T.B., Lam, S.E., Khandaker, M.U. and Bradley, D.A. (2022). Biological agents for synthesis of nanoparticles and their applications. J. King Saud Univ. Sci., 34, 101869.
17. Kandakumar, S., Sathya, V. and Manju, V. (2014). Synthesis and Characterization of Silver Nanoparticles Using *Hydnocarpus Alpina*, Its Application as A Potent Antimicrobial and Antioxidant Agent – A Novel Study. Int. J. Chem Tech Res., 6, 4770-4776.
18. Shimada, K., Fujikawa, K., Yahara, K., & Nakamura, T. (1992). Antioxidative properties of *xanthum* on the autoxidation of soybean oil in cyclodextrin emulsion. Journal of Agricultural and Food Chemistry, 40, 945–948.
19. Sun, Y. and Xia, Y. (2002) Shape-Controlled synthesis of Gold and Silver Nanoparticles. Science, 2176-2179.
20. Rout, Y., Behera, S., Ojha, A.K and Nayak P.L. (2012). Green synthesis of silver nanoparticles using *Ocimum sanctum* (Tulashi) and study of their antibacterial and antifungal activities. Journal of Microbiology and Antimicrobials, 4, 103-109.
21. Yu, F., Li, R. and Wang, R. (2004) Inhibitory effects of the *Gentiana macrophylla* extract on rheumatoid arthritis of rats. J. Ethnopharmacol, 95, 77–81.
22. Zhang, L., Wei, Y., Wang, H., Wu, F., Zhao, Y., Liu, X., Wu, H., Wang, L. and Su, H. (2020). Green synthesis of silver nanoparticles using mushroom *Flammulina velutipes* Extract and their antibacterial activity against aquatic pathogens. Food Bioprocess Technol., 13, 1908–1917.